J|A|C|S
ARTICLES
Published on Web 10/26/2004

Strong Electronic Coupling between Dimolybdenum Units Linked by the *N,N′*-Dimethyloxamidate Anion in a Molecule Having a Heteronaphthalene-like Structure

F. Albert Cotton,* Chun Y. Liu, Carlos A. Murillo,* Dino Villagrán, and Xiaoping Wang

Contribution from the Department of Chemistry and Laboratory for Molecular Structure and Bonding, P.O. Box 30012, Texas A&M University, College Station, Texas 77842-3012

Received June 1, 2004; E-mail: cotton@tamu.edu; murillo@tamu.edu

Abstract: Very strong electronic communication, manifested in a K_C value of ca. 10^9, has been found in a system of three compounds separated by one electron oxidation where each compound contains two metal−metal bonded Mo_2^{n+} units linked by a dimethyloxamidate anion, $CH_3N(O)C-C(O)NCH_3^{2-}$. The Mo−Mo distances increase as the oxidation state increases and the bond order decreases, while the diamagnetic, doubly oxidized species becomes essentially planar and resembles a naphthalene molecule. Calculations at the DFT level indicate that a strong transition in the near-IR region, shown by the singly oxidized and paramagnetic species, is best described as a HOMO−1 → SOMO transition.

1. Introduction

Mixed-valence (MV) compounds have been the subject of interest in both theoretical and experimental work[1,2] and have received a great deal of attention. This is especially true in the intersections of multidisciplinary areas, such as the search for a better understanding of some important life processes[3] where MV units are commonly found. Examples are Fe^{II}/Fe^{III} in ferridoxin, $Mn^{II}/Mn^{III}/Mn^{IV}$ clusters in photosystem II, and Cu^{I}/Cu^{II} in hemocyanin. Interest has also been sparked by the potential for development of molecular electronics and nanoscale materials[4] based on to the conductive, optical, and magnetic properties of such compounds.

Perhaps the most intensively studied systems containing MV species are those consisting formally of two potentially identical metal-containing units which differ by one electron and are linked by a group that allows the odd electron to move back and forth between the two metal centers. The earliest well-studied example is the pyrazine-bridged decaamminediruthenium ion, $[(NH_3)_5Ru(pyrazine)Ru(NH_3)_5]^{5+}$ (**I**, Chart 1), known as the Creutz−Taube (C−T) complex.[5] There are also many important dinuclear organometallic compounds where the same situation is encountered.[6] Important issues to deal with in compounds of this type are the location of the odd electron and how it is transferred from one end (donor) to the other (acceptor). In general, for compounds of this type the answer to such questions depends on the nature of the linker and thus the strength of the electronic coupling between the two linked metal units. Depending on the ability of the linker to transmit electronic communication, some species can be classified according to Robin−Day's scheme[7] as being "valence-trapped", class I compounds. In a class I compound, the two metal-containing units have different structure parameters (bond lengths and angles) that persist over many vibrational cycles, at least. In fact, to be safely assigned to class I, the rate of electron transfer from one metal center to the other should be so slow as to allow these centers to be distinguishable over much longer periods than that. At the other extreme are compounds in which the two metal centers are indistinguishable even on the time scale of electronic spectroscopy. These are truly electron-delocalized compounds that belong to class III. Everything between the extremes of class I and class III is said to

Chart 1

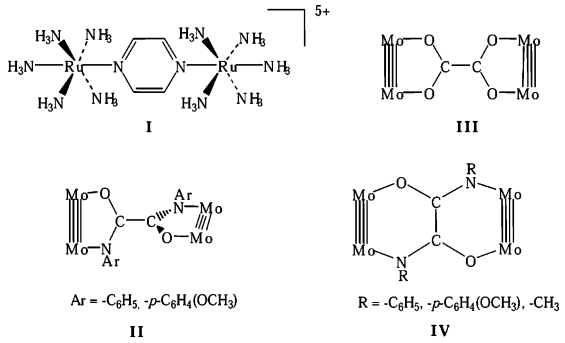

(1) (a) Brunschwig, B. S.; Sutin, N. *Coord. Chem. Rev.* **1999**, *187*, 233. (b) Bencini, A.; Ciofini, I.; Daul, C. A.; Ferretti, A. *J. Am. Chem. Soc.* **1999**, *121*, 11418. (c) Ferretti A.; Lami, A.; Murga, L. F.; Shehadi, I. A.; Ondrechen, M. J.; Villani, G. *J. Am. Chem. Soc.* **1999**, *121*, 2594. (d) Brunschwig, B. S.; Creutz, C.; Sutin, N. *Chem. Soc. Rev.* **2002**, *31*, 168.
(2) (a) Creutz, C. *Prog. Inorg. Chem.* **1983**, *30*, 1. (b) Richardson, D. E.; Taube, H. *Coord. Chem. Rev.* **1984**, *60*, 107. (c) Demadis, K. D.; Hartshorn, C. M.; Meyer, T. J. *Chem. Rev.* **2001**, *101*, 2655.
(3) Prassides, K., Ed. *Mixed-Valency Systems: Applications in Chemistry, Physics and Biology*; Kluwer Academic Publishers: Dordrecht, 1991.
(4) (a) Ward, M. D. *Chem. Soc. Rev.* **1995**, *34*, 121. (b) Astruc, D. *Acc. Chem. Res.* **1997**, *30*, 383. (c) McCleverty, J. A.; Ward, M. D. *Acc. Chem. Res.* **1998**, *31*, 842.
(5) (a) Creutz, C.; Taube, H. *J. Am. Chem. Soc.* **1969**, *91*, 3988. (b) Creutz, C.; Taube, H. *J. Am. Chem. Soc.* **1973**, *95*, 1086.
(6) See for example: Barlow, S.; O'Hare, D. *Chem. Rev.* **1997**, *97*, 637.
(7) Robin, M.; Day, P. *Adv. Inorg. Chem. Radiochem.* **1967**, *10*, 247.

10.1021/ja046775f CCC: $27.50

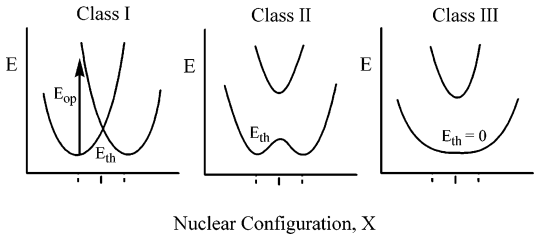

Figure 1. Potential wells for class I, class II, and class III mixed-valence compounds.

be class II (from weak coupling to the borderline of complete delocalization).[8] This classification of compounds has often been described by the diagrams shown in Figure 1.[9] For class I and class II compounds, the odd electron is trapped, to some degree, on one of the two metal centers because of the energy barrier (E_{th}) for thermal electron transfer, whereas in class III compounds, no such energy barrier is present, i.e., $E_{th} = 0$, and the odd electron is equally present on both metal centers,[1,2,9] and to some extent on atoms of the linking group.

Great efforts have been made to study analogues of the C−T complex[2,10] and to develop new coupled systems[11] which have been designed to gain more insight into the details of electronic coupling and how to control the extent of electronic communication between the two mononuclear metal centers. In nearly all of these previous cases with two single-metal-atom components, the C−T ion being most prominent but in no way an atypical example, direct structural evidence bearing on the question of delocalization (or lack thereof) has been unavailable, despite assiduous and skillful efforts to obtain it. This is because the missing electron at the oxidized end has been removed from an essentially nonbonding orbital so that little in the way of structural change is to be expected. It is no surprise, therefore, that nothing conclusive is seen.[12] Structural efforts are further hampered by the fact that bond distances between metal atoms and light ligand atoms (typically N or C) are bound to have relatively high estimated standard deviations, and chemically equivalent but crystallographically inequivalent ones on the two ends may differ by about as much as would be expected to result from oxidation state differences. In summary, few if any of the mixed-oxidation-state species that have been subjected to extreme scrutiny by spectroscopic methods could be considered good subjects for structural study.

In this laboratory we have set as our goal to design, synthesize, and study MV compounds that can be studied by all of the (mainly spectroscopic) techniques previously used for such research, but that can also, *with every expectation of definitive results*, be studied structurally, i.e., by X-ray crystallography. To do this we have employed covalently bonded dimetal units instead of mononuclear metal units. Typically we have used compounds of the type $[Mo_2]L[Mo_2]$, where $[Mo_2]$ is an abbreviation for an Mo_2^{4+} unit embraced by three *N*,*N*′-di(*p*-anisyl)formamidinate (DAniF) anions, that is $[Mo_2(DAniF)_3]^+$, and L is a dicarboxylate anion[13] or a tetrahedral anion such as EO_4^{2-} (E = S, Mo, W).[14] Generally, electrochemical studies have shown that these compounds exhibit two reversible redox couples corresponding to the two one-electron oxidation processes occurring at each of the $[Mo_2]$ units.[13,14]

There are two important advantages in having compounds with two dimetal centers for the study of MV species. First, the electronic properties of many dimetal units are simple and well established. This is particularly true for multiply bonded Mo_2 units[15] which have a $\sigma^2\pi^4\delta^2$ or a $\sigma^2\pi^4\delta$ configuration. The change of one δ electron can be tracked unambiguously in the metal−metal bond distance and the position of the $\delta \rightarrow \delta^*$ transitions in the electronic spectra.[16]

Prior work with dicarboxylate-linked dimolybdenum compounds $[Mo_2]L[Mo_2]$ ($L = O_2C\text{-}X\text{-}CO_2$) has revealed that the orbital interactions between the δ orbitals of the $[Mo_2]$ units and the π^* orbitals of the linker are significant enough to engender some degree of electron delocalization over the two $[Mo_2]$ units. However, electrochemical studies[17] show that, in general, dicarboxylate linkers afford relatively weak coupling between the two $[Mo_2]$ units, and these compounds belong to class II or, even more often, to class I.[13b] In our search for more strongly coupled and robust systems, the more basic diamidate anions were chosen for the linking of $[Mo_2]$ units.[18,19] Previously[19] we found that *N*,*N*′-diaryloxamidate anions bridge between two $[Mo_2]$ units in two different ways, referred to as α and β. In the α form, **II** (Chart 1), the C−C bond of the oxamidate anion is nearly perpendicular to the Mo−Mo bonds, as it is in the case of the oxalate, **III**, and there are two five-membered rings $\overline{\text{Mo−Mo−N−C−O}}$ connected by a C−C single bond. There is an important difference between **II** and **III**, however, in that the oxalate structure is planar, whereas in **II** the Mo−Mo units are perpendicular to each other. In the β form, **IV** (which has no known oxalate analogue), the two Mo−Mo bonds and the C−C bond are roughly parallel and two six-membered $\overline{\text{Mo−Mo−N−C−C−O}}$ rings sharing a C−C bond are present. With the β bridging mode, in which the two $[Mo_2]$ units form opposite edges of two fused, six-membered rings, the electronic coupling between the two $[Mo_2]$ units is much greater than with the α mode. The comproportionation constant, K_C, of ca. 10^9 for the process in eq 1 is 3−5 orders of

$$[Mo_2^{5+}]L[Mo_2^{5+}] + [Mo_2^{4+}]L[Mo_2^{4+}] \rightleftharpoons 2[Mo_2^{5+}]L[Mo_2^{4+}] \quad (1)$$

magnitude greater than those in compounds with dicarboxylate linkers. This suggests that the β-oxamidate compounds should

(8) See for example: Nelsen, S. F. *Chem. Eur. J.* **2000**, *6*, 581 and references therein.
(9) (a) Hush, N. S. *Prog. Inorg. Chem.* **1967**, *8*, 391. (b) Sutin, N. *Prog. Inorg. Chem.* **1983**, *30*, 441. (c) Crutchley, R. J. *Adv. Inorg. Chem.* **1994**, *41*, 273. (d) Sutin, N. *Adv. Chem. Phys.* **1999**, *106*, 7.
(10) (a) Sutton, J. E.; Taube, H. *Inorg. Chem.* **1981**, *20*, 3125. (b) Joss, S.; Bürgi, H. B.; Ludi, A. *Inorg. Chem.* **1985**, *24*, 949. (c) Lay, P. A.; Magnuson, R. H.; Taube, H. *Inorg. Chem.* **1988**, *27*, 2364. (d) Ito, T.; Hamaguchi, T.; Nagino, H.; Yamaguchi, T.; Kido, H.; Zavarine I. S.; Richmond, T.; Washington, J.; Kubiak, C. P. *J. Am. Chem. Soc.* **1999**, *121*, 4625. (e) Mosher, P. J.; Yap, G. P. A.; Crutchley, R. J. *Inorg. Chem.* **2001**, *40*, 1189.
(11) (a) Demadis, K. D.; Neyhart, G. A.; Kober, E. M.; Meyer, T. J. *J. Am. Chem. Soc.* **1998**, *120*, 7121. (b) Demadis, K. D.; Neyhart, G. A.; Kober, E. M.; White, P. S.; Meyer, T. J. *Inorg. Chem.* **1999**, *38*, 5948. (c) Kaim, W.; Klein, A.; Glöckle, M. *Acc. Chem. Res.* **2000**, *33*, 755. (d) Atwood, C. G.; Geiger, W. E. *J. Am. Chem. Soc.* **2000**, *122*, 5477.
(12) (a) Fürholz, U.; Bürgi, H.-B.; Wagner, F. E.; Stebler, A.; Ammeter, J. H.; Krausz, E.; Clark, R. J. H.; Stead, M. J.; Ludi, A. *J. Am. Chem. Soc.* **1984**, *106*, 121. (b) Fürholz, U.; Joss, S.; Bürgi, H.-B.; Ludi, A. *Inorg. Chem.* **1985**, *24*, 943.
(13) (a) Cotton, F. A.; Donahue, J. P.; Lin, C.; Murillo, C. A. *Inorg. Chem.* **2001**, *40*, 1234. (b) Cotton, F. A.; Donahue, J. P.; Murillo, C. A. *J. Am. Chem. Soc.* **2003**, *125*, 5436. (c) Cotton, F. A.; Donahue, J. P.; Murillo, C. A.; Pérez, L. M. *J. Am. Chem. Soc.* **2003**, *125*, 5486.
(14) Cotton, F. A.; Donahue, J. P.; Murillo, C. A. *Inorg. Chem.* **2001**, *40*, 2229.
(15) Cotton, F. A.; Walton, R. A. *Multiple Bonds between Metal Atoms*, 2nd ed.; Oxford University Press: Oxford, 1993.

fall into the delocalized class III category. In contrast, the α-oxamidate analogues show relatively poor coupling of the $[Mo_2]$ units, with K_C's of about 10^3.[19] This set of arylamidato-bridged compounds exemplifies the switching of electronic localization/delocalization by configurational control.

Recently, we also reported the isolation and structural characterization of a series of compounds of the type $[Mo_2]M(OCH_3)_4[Mo_2]^{n+}$ ($n = 0$, 1, or 2 for M = Zn; $n = 0$ or 1 for M = Co).[20] In these compounds, the two $[Mo_2]$ units are essentially perpendicular to each other like those in the α form, and for those with $n = 1$, the unpaired electron is trapped on one of the $[Mo_2]$ units. This was shown by crystallography as two unambiguously distinguishable Mo−Mo distances of ca. 2.11 and 2.15 Å for the Mo_2^{4+} and Mo_2^{5+} units, respectively. The Mo−N distances also show the effect of the electron localization (also called valence-trapping), with those on the oxidized unit being shorter than those in the nonoxidized species.[20b] We have also reported the first electron-delocalized compound having dimolybdenum units in $\{[Mo_2(DAniF)_2]_2(\mu\text{-}Cl_4)\}PF_6$, which features a very short $[Mo_2]\cdots[Mo_2]$ separation (ca. 3.6 Å) and has the odd electron delocalized over both $[Mo_2]$ units,[21] with both of the Mo−Mo distances being 2.1453(3) Å. The electron localization found crystallographically in tetramethoxyzincate and -cobaltate, and the delocalization in the compound bridged by the four chloride anions, are consistent with predictions from electrochemical measurements in solution.[20b,21]

The compounds with *N*,*N*′-diaryloxamidato bridges were important in showing the structure dependence of electron coupling, because for the α structure the K_C values are only about 10^3, whereas for the β structure the K_C values are about 10^9. However, there were experimental difficulties, which we are trying to overcome, in obtaining the oxidized forms of these *N*,*N*′-diaryl compounds in crystalline form, and therefore structural evidence for valence-trapped or delocalized character has not yet been obtained. In the meantime we have turned to the *N*,*N*′-dimethyloxamidate compound. While there is no evidence for the formation of an α isomer, though it might be a fleeting kinetic product, the β isomer can be obtained in good yield, and it resembles the β isomers of the aryloxamidato compounds in having a K_C value of about 10^9.

Here we report a series of *N*,*N*′-dimethyloxamidate-linked dimolybdenum pairs $\{[Mo_2](oxamidate)[Mo_2]\}^{n+}$ ($n = 0$, 1, and 2). The procedure entailed the following: (1) reaction of $Mo_2(DAniF)_3(O_2CCH_3)$ (where DAniF is the anion of *N*,*N*′-di-(*p*-anisyl)formamidine) with $CH_3(H)N(O)C-C(O)N(H)CH_3$ and sodium methoxide to give the neutral molecule; (2) one-electron oxidation; and (3) two-electron oxidation with ferrocenium hexafluorophosphate to give the mono- and dications as their PF_6^- salts. In all three of these compounds, the two $[Mo_2]$ units and the linker are almost planar, with the linker in the β coordination mode, **IV**, and the two Mo−Mo bonds nearly parallel to each other. For the MV complex there is strong electronic communication, as shown by a HOMO−1 to SOMO band in the near-IR spectrum. The existence of three compounds in this family allows the analysis and comparison of molecular structural features, electrochemical behavior, and magnetic and spectroscopic properties. Furthermore, density functional theory (DFT) calculations provide further insight into their electronic structures and physical properties. The compounds are $[Mo_2(DAniF)_3]_2$(oxamidate) (**1**), $\{[Mo_2(DAniF)_3]_2(oxamidate)\}PF_6$ (**2**), and $\{[Mo_2(DAniF)_3]_2(oxamidate)\}(PF_6)_2$ (**3**), in which oxamidate is the dianion $CH_3N(O)CC(O)NCH_3$ in its β bridging mode.

2. Experimental Section

Materials and Methods. Solvents were purified under argon using a Glass Contour solvent purification system or distilled under nitrogen. All synthetic operations were conducted under N_2 using Schlenk line techniques. The starting material $Mo_2(DAniF)_3(O_2CCH_3)$ was prepared by following a published method;[19] commercially available chemicals were used as received.

Physical Measurements. Elemental analyses were performed by Canadian Microanalytical Service (Delta, British Columbia, Canada). Electronic spectra of **1**, **2**, and **3** in CH_2Cl_2 were measured in a range of 300−800 nm on a Shimadzu UV-2501PC spectrophotometer or on a Cary 17 in the 800−3000 nm range. ^{1}H NMR spectra were recorded on a Mercury-300 NMR spectrometer with chemical shifts (δ ppm) referenced to $CDCl_3$. The electrochemical measurements were recorded on a CH Instruments electrochemical analyzer with Pt working and auxiliary electrodes, Ag/AgCl reference electrodes, scan rate of 100 mV/s, and 0.1 M Bu_4NPF_6 (in CH_2Cl_2) as electrolyte. Under these experimental conditions, the $E_{1/2}(Fc^+/Fc)$ was measured at 440 mV. Magnetic susceptibility measurements were performed on a Quantum Design SQUID MPMS-XL magnetometer, and the EPR spectra were recorded using a Bruker ESP300 spectrometer.

Computational Details. DFT[22] calculations were performed with the hybrid Becke-3[23] parameter exchange functional and the Lee−Yang−Parr[24] nonlocal correlation functional (B3LYP) implemented in the Gaussian 98 program suite.[25] Double-ζ-quality basis sets (D95)[26] were used on nonmetal atoms (carbon, nitrogen, oxygen, and hydrogen). A small (1s2s2p3s3p3d) effective core potential (ECP)[27] was used for the molybdenum atoms along with the associated double-ζ basis set (LANL2DZ). The convergence criterion for the self-consistent field cycles on all calculations was increased from the default value to 10^{-8}. The Becke−Perdew[28,29] functional (BP86) was employed for compari-

(16) See for example: (a) Cotton, F. A.; Hillard, E. A.; Murillo, C. A. *Inorg. Chem.* **2002**, *41*, 1639. (b) Cotton, F. A.; Daniels, L. M.; Murillo, C. A.; Timmons, D. J.; Wilkinson, C. C. *J. Am. Chem. Soc.* **2002**, *124*, 9249. (c) Cotton, F. A.; Huang, P.; Murillo, C. A.; Wang, X. *Inorg. Chem. Commun.* **2003**, *6*, 121.
(17) Richardson, D. E.; Taube, H. *Inorg. Chem.* **1981**, *20*, 1278.
(18) Cotton, F. A.; Daniels, L. M.; Donahue, J. P.; Liu, C. Y.; Murillo, C. A. *Inorg. Chem.* **2002**, *41*, 1354.
(19) Cotton, F. A.; Liu, C. Y.; Murillo, C. A.; Villagrán, D.; Wang, X. *J. Am. Chem. Soc.* **2003**, *125*, 13564.
(20) (a) Cotton, F. A.; Liu, C. Y.; Murillo, C. A.; Wang, X. *Inorg. Chem.* **2003**, *42*, 4619. (b) Cotton, F. A.; Dalal, N. S.; Liu, C. Y.; Murillo, C. A.; North, J. M.; Wang, X. *J. Am. Chem. Soc.* **2003**, *125*, 12945.
(21) Cotton, F. A.; Liu, C. Y.; Murillo, C. A.; Wang, X. *Chem. Commun.* **2003**, 2190.
(22) (a) Hohenberg, P.; Kohn, W. *Phys. Rev.* **1964**, *136*, B864. (b) Parr, R. G.; Yang, W. *Density-Functional Theory of Atoms and Molecules*; Oxford University Press: Oxford, 1989.
(23) (a) Becke, A. D. *Phys. Rev. A* **1988**, *38*, 3098. (b) Becke, A. D. *J. Chem. Phys.* **1993**, *98*, 1372. (c) Becke, A. D. *J. Chem. Phys.* **1993**, *98*, 5648.
(24) Lee, C. T.; Yang, W. T.; Parr, R. G. *Phys. Rev. B* **1998**, *37*, 785.
(25) Frisch, M. J.; Trucks, G. W.; Schlegel, H. B.; Scuseria, G. E.; Robb, M. A.; Cheeseman, J. R.; Zakrzewski, V. G.; Montgomery, J. A.; Stratmann, R. E.; Burant, J. C.; Dapprich, S.; Millam, J. M.; Daniels, A. D.; Kudin, K. N.; Strain, M. C.; Farkas, O.; Tomasi, J.; Barone, V.; Cossi, M.; Cammi, R.; Mennucci, B.; Pomelli, C.; Adamo, C.; Clifford, S.; Ochterski, J.; Petersson, G. A.; Ayala, P. Y.; Cui, Q.; Morokuma, K.; Malick, D. K.; Rabuck, A. D.; Raghavachari, K.; Foresman, J. B.; Cioslowski, J.; Ortiz, J. V.; Stefanov, B. B.; Liu, G.; Liashenko, A.; Piskorz, P.; Komaromi, I.; Gomperts, R.; Martin, R. L.; Fox, D. J.; Keith, T.; Al-Laham, M. A.; Peng, C. Y.; Nanayakkara, A.; Gonzalez, C.; Challacombe, M.; Gill, P. M. W.; Johnson, B. G.; Chen, W.; Wong, M. W.; Andres, J. L.; Head-Gordon, M.; Replogle, E. S.; Pople, J. A. *Gaussian 98*, revision A.9; Gaussian, Inc.: Pittsburgh, PA, 1998.
(26) Dunning, T. H.; Hay, P. J. In *Modern Theoretical Chemistry*. *3. Methods of Electronic Structure Theory*; Schaefer, H. F., III, Ed.; Plenum Press: New York, 1977; pp 1−28.
(27) (a) Wadt, W. R.; Hay, P. J. *J. Chem. Phys.* **1985**, *82*, 284. (b) Wadt, W. R.; Hay, P. J. *J. Chem. Phys.* **1985**, *82*, 299.
(28) Becke, A. D. *Phys. Rev. A* **1988**, *38*, 3098.
(29) Perdew, J. P. *Phys. Rev. B* **1986**, *33*, 8822.

son to B3LYP results. Time-dependent density functional (TD-DFT) calculations[30] were performed using the Gaussian program suite. All calculations were done on either an Origin 2000 32-processor or an Origin 3800 64-processor SGI computer located at the Texas A&M supercomputing facility.

Preparation of β-[Mo_2(DAniF)$_3$]$_2$[CH_3N(O)CC(O)NCH_3], 1. To a mixture of Mo_2(DAniF)$_3$(O_2CCH_3) (1.02 g, 1.00 mmol) and *N*,*N*′-dimethyloxamide (0.058 g, 0.50 mmol) was added 30 mL of THF, and then 2.0 mL of a 0.5 M solution of $NaOCH_3$ in methanol. The yellow color changed to red upon addition of the base. The mixture was stirred at room temperature overnight and an orange-red solid formed. The supernatant liquid was decanted, and the solid was washed with 15 mL of ethanol, followed by 20 mL of hexanes. The solid was dried under vacuum and then extracted with dichloromethane (ca. 20 mL). The resulting mixture was passed through a Celite-packed frit to remove some insoluble NaO_2CCH_3. The volume of the filtrate was reduced under vacuum to ca. 10 mL. Next 50 mL of ethanol was added, producing an orange-red precipitate. The solid was collected by filtration and dried under vacuum. Yield: 0.75 g (74%). ^{1}H NMR at 25 °C (δ ppm in $CDCl_3$): 8.43 (vb, 6H, −NC*H*N−), 6.59)6.41 (m, 28H, aromatic C−*H*), 6.35 (d, 8H, aromatic C−*H*), 6.28 (d, 4H, aromatic C−*H*), 6.21 (d, 4H, aromatic C−*H*), 6.05 (d, 4H, aromatic C−*H*), 3.70 (s, 6H, −OCH_3), 3.68 (s, 12H, −OCH_3), 3.60 (s, 12H, −OCH_3), 3.56 (s, 6H, −OCH_3), 2.12 (b, 6H, −CH_3). ^{1}H NMR at −50 °C (δ ppm in $CDCl_3$): 8.44 (s, 4H, −NC*H*N−), 8.24 (s, 2H, −NC*H*N−), 6.61 (d, 8H, aromatic C−*H*), 6.55−6.50 (m, 12H, aromatic C−*H*) 6.46 (d, 8H, aromatic C−*H*), 6.32 (d, 8H, aromatic C−*H*), 6.25 (d, 4H, aromatic C−*H*), 6.16 (d, 4H, aromatic C−*H*), 5.96 (d, 4H, aromatic C−*H*), 3.71 (s, 6H, −OCH_3), 3.70 (s, 12H, −OCH_3), 3.62 (s, 12H, −OCH_3), 3.57 (s, 6H, −OCH_3), 2.18 (s, 6H −CH_3). UV−vis, λ_{max} (ϵ, M^{-1} mol^{-1}): 441 nm (2.2×10^3), 495 nm (2.3×10^3). Anal. Calcd for $C_{94}H_{96}Mo_4N_{14}O_{14}$: C, 55.63; H, 4.77; N, 9.66. Found: C, 55.86; H, 4.73; N, 9.35.

Preparation of β-{[Mo_2(DAniF)$_3$]$_2$[CH_3N(O)CC(O)NCH_3]}PF_6, 2. Solutions of **1** (0.304 g, 0.150 mmol) in 10 mL of CH_2Cl_2 and ferrocenium hexafluorophosphate (0.050 g, 0.150 mmol) in 20 mL of CH_2Cl_2 were prepared separately and cooled to −78 °C. Upon addition of the solution containing the oxidizing agent to that of the neutral complex, the color of the solution changed from red to dark brown. This solution was stirred at low temperature for 30 min, and 50 mL of hexanes was then added by syringe to produce a dark-brown precipitate. The supernatant liquid was decanted and the solid was washed with 20 mL of cold (ca. 0 °C) hexanes. The solid was dissolved in 15 mL of dichloromethane, and the solution was layered with 45 mL of hexanes. After two weeks of diffusion, dark-brown crystals were collected. Yield: 0.25 g (77%). UV−vis, λ_{max} (ϵ, M^{-1} mol^{-1}): 432 nm (1.0×10^3), 568 nm (1.6×10^3), 800 nm (3.5×10^2). Anal. Calcd for $C_{94}H_{96}F_6Mo_4N_{14}O_{14}P$: C, 51.92; H, 4.45; N, 9.02. Found: C, 52.13; H, 4.43; N, 8.72.

Preparation of β-{[Mo_2(DAniF)$_3$]$_2$[CH_3N(OCC(O)NCH_3]}-(PF_6)$_2$, 3. This was made similarly to **2** but by mixing a solution of **1** (0.406 g, 0.200 mmol) in 10 mL of CH_2Cl_2 with a solution of ferrocenium hexafluorophosphate (0.140 g, 0.422 mmol) in 20 mL of CH_2Cl_2. Upon transferring the oxidizing agent to the red Mo_2 complex at −78 °C, the color changed to dark-brown. After this solution was stirred at low temperature for 30 min, 50 mL of hexanes was added to produce a very dark-brown precipitate. The supernatant liquid was then decanted and the solid residue was washed with 20 mL of precooled hexanes. The solid was dissolved in ca. 20 mL of dichloromethane, and the solution was layered with 45 mL of hexanes to give large, almost black crystals that were collected after two weeks of diffusion. Yield: 0.42 g (90%). ^{1}H NMR at 25 °C (δ ppm in $CDCl_3$): 6.86 (d, 8H, aromatic C−*H*), 6.76 (d, 4H, aromatic C−*H*), 6.59 (d, 8H, aromatic C−*H*), 6.44 (d, 8H, aromatic C−*H*), 6.42 (d, 8H, aromatic C−*H*), 6.32 (d, 8H, aromatic C−*H*), 6.12 (d, 4H, aromatic C−*H*), 3.78 (s, 6H, −OCH_3), 3.73 (s, 12H, −OCH_3), 3.64 (s, 12H, −OCH_3), 3.60 (s, 6H, −OCH_3), 2.86 (b, 6H, −CH_3). ^{1}H NMR at −50 °C (δ ppm in $CDCl_3$): 8.60 (b, 6H, −NC*H*N−), 6.90 (d, 8H, aromatic C−*H*), 6.76 (d, 4H, aromatic C−*H*), 6.62 (d, 8H, aromatic C−*H*), 6.40 (d, 8H, aromatic C−*H*), 6.37 (d, 8H, aromatic C−*H*), 6.31 (d, 8H, aromatic C−*H*), 6.12 (d, 4H, aromatic C−*H*), 3.79 (s, 6H, −OCH_3), 3.75 (s, 12H, −OCH_3), 3.64 (s, 12H, −OCH_3), 3.63 (s, 6H, −OCH_3), 2.76 (b, 6H, −CH_3). UV−vis, λ_{max} (ϵ, M^{-1} mol^{-1}): 464 nm (1.3×10^3), 600 nm (5.1×10^2), 800 nm (2.3×10^3). Anal. Calcd for $C_{94}H_{96}F_{12}Mo_4N_{14}O_{14}P_2$: C, 48.67; H, 4.17; N, 8.45. Found: C, 48.72; H, 4.08; N, 8.45.

X-ray Structure Determinations. Single crystals were grown by diffusion of hexanes into solutions of **1** in dichloroethane, **2** in THF, and **3** in dichloromethane. For each of the three compounds, a crystal suitable for X-ray diffraction analysis was attached to the tip of a quartz fiber with a small amount of silicone grease and then placed on a goniometer head. Data for **1**·4CH_2ClCH_2Cl, **2**·6C_4H_8O, and **3**·3CH_2Cl_2 were collected at 213 K on a Bruker SMART 1000 CCD system equipped with a low-temperature controller cooled by liquid nitrogen. In each case, 20 frames were collected first to determine the orientation matrix. The cell parameters were calculated using an autoindexing routine and then a hemisphere of data was gathered. During the course of data collection, no crystal decay was observed. Data reduction and integration were performed with the software package SAINT,[31] which corrects for Lorentz and polarization effects, while absorption corrections were applied by using the program SADABS.[32]

The crystals of **2**·6THF were twinned by a 180° rotation about reciprocal axis [010] and followed the twin law:

$$h_2 = \begin{bmatrix} -1.0000 & 0.0000 & 0.0000 \\ -0.2556 & 1.0000 & -0.2499 \\ 0.0000 & 0.0007 & -1.0000 \end{bmatrix} h_1$$

where h_1 and h_2 are the orientation matrices for the two twin components. Data were processed with the SAINT software.[31] Absorption corrections were applied with the program TWINABS.[33] The data were transformed to SHELX HKLF 5 format so that both twin components could be refined simultaneously. Positions of non-hydrogen atoms for all compounds were found by using the direct methods program in the Bruker SHELXTL software package.[34] Subsequent cycles of least-squares refinement followed by difference Fourier syntheses revealed the positions of the remaining non-hydrogen atoms. Hydrogen atoms were placed in calculated positions in the final structure refinement. Crystal data and structural refinement information for **1**·4CH_2ClCH_2Cl, **2**·6C_4H_8O, and **3**·3CH_2Cl_2 are in Table S1. Selected distances and angles are given in Table S2.

3. Results and Discussion

Syntheses. The neutral compound **1** was prepared following our recently developed method for making oxamidate-bridged dimolybdenum compounds by reacting Mo_2(DAniF)$_3$(O_2CCH_3) with *N*,*N*′-dimethyloxamide and $NaOCH_3$ in THF according to eq 2. Although a few diamidate-linked dimetal pairs have been

$$2Mo_2(DAniF)_3(O_2CCH_3) + CH_3(H)N(O)C{-}C(O)N(H)CH_3 + 2NaOCH_3 \rightarrow [Mo_2(DAniF)_3]_2CH_3N(O)C{-}C(O)NCH_3 + 2NaO_2CCH_3 + 2CH_3OH \quad (2)$$

reported,[18,19,35] the synthetic methodology has not previously

(30) Casida, M. E.; Jamorski, C.; Casida, K. C.; Salahub, D. R. *J. Chem. Phys.* **1998**, *108*, 4439.

(31) *SAINT. Data Reduction Software. Version 6.36A*; Bruker Analytical X-ray Systems, Inc.: Madison, WI, 2002.

(32) *SADABS. Bruker/Siemens Area Detector Absorption and Other Corrections. V2.03*; Bruker Analytical X-ray Systems, Inc.: Madison, WI, 2002.

been generalized, and several aspects of the present synthesis merit comment. The use of the mixed-ligand starting material $Mo_2(DAniF)_3(O_2CCH_3)$ is essential for the success of the reaction because $[Mo_2(DAniF)_3(CH_3CN)_2]BF_4$, which has been used widely to make dicarboxylate analogues, did not produce any isolable products.

The one-pot reaction outlined in eq 2 gives a product that can be readily purified because the solid byproduct, NaO_2CCH_3, can be removed conveniently by filtration to give **1** in good yield and high purity. We believe that with appropriate modifications, this procedure might be a general one for the preparation of species with other dimetal units. It is important to note that when the oxamidate RN(O)C−C(O)NR ligand contains a bulky aryl group, such as phenyl or anisyl,[19] an additional step is necessary to isolate the product. Moreover, depending on the conditions, one of two isomers can be obtained, either the α or the β form, with the former being isolated in higher yield and better purity.[19] Interestingly, when R = CH_3, the reaction yields exclusively the β-dimethyloxamidate analogue in one step, and no α isomer is observed. It appears that, in the present case, the β form is thermodynamically so highly favored over the α form that the α isomer, which might be kinetically preferred, is too quickly converted to the β form to allow its isolation, or even to signal its transient presence, contrary to what was found with the N-aryl compounds.[19]

Compounds **2** and **3** were prepared by oxidizing the neutral precursor **1** with 1 or 2 equiv of ferrocenium hexafluorophosphate, respectively, which yields ferrocene as a byproduct that can be easily removed by washing with hexanes. The reactions are essentially quantitative, but rigorous control of the stoichiometry and low reaction temperatures are necessary. All three compounds are soluble in CH_2Cl_2, dichloroethane, and THF, with **1** being soluble also in less polar solvents such as toluene and benzene. It should be noted that isolation of oxidized species having one Mo_2^{5+} unit has been rather difficult and that we have not succeeded yet in isolating cations of the types $[Mo_2]$-(dicarboxylate)$[Mo_2]^{n+}$. Success with the oxamidate analogues appears to be due to the high stabilization of the oxidized species by the very basic linkers. For comparison, the electrode potentials of the first one-electron oxidation process are almost 463 mV lower for the oxamidate pairs than for the oxalate analogue (vide infra). This allows the use of the mild oxidizing agent ferrocenium hexafluorophosphate for the one- and two-electron oxidations of the neutral molecule.

Structural and NMR Results. Preparation of single crystals for structural analysis of the series of three compounds was challenging. This was especially true for **2**, where after many attempts using a variety of experimental conditions, it was found that diffusion of hexanes into THF solutions gave the best crystals.

Compound **1** crystallizes in the space group $P2_1/c$ with the molecule residing on a general position. The core, depicted in Figure 2, shows that the $[Mo_2]$ units and the linker form two fused six-membered rings. This coordination mode of the

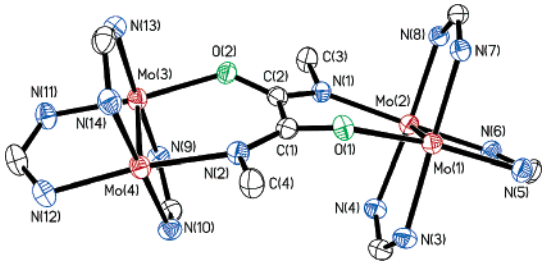

Figure 2. Core of **1** in **1**·4CH_2ClCH_2Cl drawn with 40% probability ellipsoids. All *p*-anisyl groups and hydrogen atoms have been omitted for clarity.

oxamidate linker, designated as β, has been seen previously in two diaryloxamidate-linked analogues. In an idealized form of this β binding mode, the two Mo−Mo bonds and the C−C bond would be coplanar and almost parallel to each other. The torsion angles defined by N(1)−C(1)−C(2)−N(2) and O(1)−C(1)−C(2)−O(2) are 22.7° and 32.8°, respectively, and there is a dihedral angle of 161°. The Mo−Mo bond distances obtained for the two crystallographically independent $[Mo_2]$ units, 2.0898(5) and 2.0910(5) Å, are identical within their esd's, and fall in the range for quadruply bonded Mo−Mo units having a $\sigma^2\pi^4\delta^2$ electronic configuration, and supported by similar ligands.[19,36] These Mo−Mo bond lengths are essentially the same as that of 2.0892(8) Å found in the starting material $Mo_2(DAniF)_3$-(O_2CCH_3). The replacement of the acetate anion by an oxamidate anion and the formation of the product do not affect the metal−metal bond distances. The C−C bond distance in the oxamidate bridge, 1.518(5) Å, corresponds to a single bond.

The ^1H NMR spectra show that **1** is diamagnetic. It is notable that the signals for the methine protons of the DAniF ligands, which are expected to be in the region of δ 8−9 ppm and in the ratio of 2:1 for the cis and trans formamidinate groups, are very broad and not resolved in the room-temperature spectrum, but they appear as two sharp signals in a 2:1 ratio at low temperatures, which indicates that there is a dynamic process going on in solution. This behavior, which is much like that observed in the β form of the diaryloxamidate analogues, is not yet understood and still under study. The electronic spectrum shows a $\delta \rightarrow \delta^*$ transition at 441 nm, which is in the region of other quadruply bonded Mo_2^{4+} with similar environments.[19,36]

The doubly oxidized **3** crystallizes in the triclinic space group $P\bar{1}$, with the molecule occupying a special position and having the midpoint of the central C−C bond of the linker on an inversion center. Therefore, the two $[Mo_2]$ units are crystallographically equivalent. While the core of the cation, which is shown in Figure 3, is qualitatively similar to that in **1**, in the dication the two Mo−Mo bonds and the oxamidate anion are essentially coplanar. From the small displacement ellipsoids of the core atoms, it is clear that there is no crystallographic disorder, and we conclude that the molecule is intrinsically flat; that is, the core has C_{2h} and not simply C_i symmetry. The Mo−Mo bond distances have been lengthened upon oxidation by ca. 0.04 Å to 2.1306(3) Å from 2.0904(5) Å in **1**. A Mo−Mo bond distance of 2.131 Å is typical of those found in other dimolybdenum compounds having Mo_2^{5+} units.[16,37] Clearly, upon oxidation, one electron has been removed from

(33) *TWINABS. Bruker Nonius Scaling and Corrections for Twinned Crystals. Version 1.00*; Bruker Analytical X-ray Systems, Inc.: Madison, WI, 2002.
(34) Sheldrick, G. M., *SHELXTL. Version 6.12*; Bruker Analytical X-ray Systems, Inc.: Madison, WI, 2000.
(35) Nelson, K. J.; McGaff, R. W.; Powell, D. R. *Inorg. Chim. Acta* **2000**, *304*, 130.
(36) Lin, C.; Protasiewicz, J. D.; Smith, E. T.; Ren, T. *Inorg. Chem.* **1996**, *35*, 6422.
(37) Cotton, F. A.; Feng, X.; Matusz, M. *Inorg. Chem.* **1989**, *28*, 594.

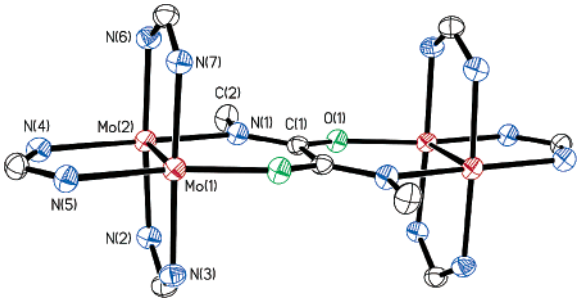

Figure 3. Cation of **3** in **3**·$3CH_2Cl_2$ drawn with 40% probability ellipsoids. All *p*-anisyl groups and hydrogen atoms have been omitted for clarity.

each of the two [Mo_2] units to give a doubly oxidized species that is crystallographically and electronically symmetrical.

The ^{1}H NMR spectrum taken at room temperature initially showed relatively broad signals, but these sharpened significantly upon addition of a small amount of iodine, which oxidized a small amount of **2** present as an impurity. This indicates that the molecule is diamagnetic (vide infra), but the resonances from the methine protons are absent just as they were in **1**. As the temperature was lowered to −50 °C, these signals began to appear. It is also noticeable that the signals for the amide methyl groups at 2.76 ppm are displaced toward lower field relative to those of **1**.

The MV compound **2** crystallizes in the triclinic space group $P\bar{1}$ with the monocation residing on a general position. The overall structure of the cation in **2** resembles more closely that of molecule **1** than that of the cation in **3**, as shown in Figure S1. The core structure, that is, the two [Mo_2] units and the oxamidate anion, is bent with a dihedral angle of 160°. It is also twisted in the same way as compound **1**, but slightly less so, with torsion angles N(1)−C(1)−C(2)−N(2) and O(1)−C(1)−C(2)−O(2) of 18.4° and 27.7°, respectively. Avoidance of crystallographic disorder in the core structure required careful selection of the solvents (THF/hexanes) used for growing crystals.[38] The two crystallographically independent Mo−Mo bond distances of 2.105(1) and 2.112(1) Å are essentially the same according to the conventional 3σ criterion for random error. Importantly, they are longer than those of **1** but shorter than those of the doubly oxidized species **3**, which indicates that the metal−metal bond order in each of the two [Mo_2] units is intermediate between those of 4.0 in **1** and 3.5 in **3**. The structure of the cation in **2** differs from those recently reported for the electronically localized MV species [Mo_2]M(OCH_3)$_4$[Mo_2]$^+$ (M = Zn, Co), which have two structurally distinct [Mo_2] units, with bond orders of 3.5 and 4.0.[20b] The lengthening of 0.015−0.021 Å in each Mo−Mo bond distance, resulting from the shared one-electron oxidation process, is similar to the change in bond distance, 0.026 Å, observed in the electron-delocalized compound [Mo_2]$^{0.5+}$(μ-Cl)$_4$[Mo_2]$^{0.5+}$.[21]

From electrostatic considerations, it is expected that as the positive charge on the dimetal centers increases, the Mo−ligand bond lengths should become shorter, and this is observed. The Mo−O_{linker} bond lengths are 2.105(2), 2.056(8), and 2.025(2) Å, and the Mo−N_{linker} bond distances are 2.173(3), 2.141(9), and 2.114(2) Å for **1**, **2**, and **3**, respectively. A similar trend is observed for the Mo−N_{DAniF} bond distances. The average Mo−N_{trans} distances are 2.131(4), 2.121(9), and 2.118(2) Å, and the Mo−N_{cis} distances are 2.155(4), 2.141(9), and 2.130(3) Å, again for **1**, **2**, and **3** in that order. The nonbonding separations between the two Mo_2 centers, 6.248 Å for **1** and 6.177 Å for **2**, are virtually the same, as expected from the similar degrees of deviation from planarity in their cores. Compound **3** has the longest Mo_2···Mo_2 distance of 6.326 Å, consistent with the presence of an essentially flat core. It might also be noted that the oxamidate C−C distances for the three compounds are the same within experimental uncertainty, viz., 1.518(5) Å for the neutral compound **1**, 1.522(12) Å for **2**, and 1.508(5) Å for **3**. Table 1 lists some important bond distances in the three compounds. It is clear that in **2**, the two dimetal units are structurally equivalent and the molecule is symmetrical (i.e., delocalized) in the solid state. On this basis, a formal bond order of 3.75 can be assigned to each of the two electronically equivalent Mo_2 units. Compounds **1**−**3** represent a rare example of linked units in which the neutral, singly oxidized, and doubly oxidized species have been structurally characterized and electronic communication between metal centers has been studied.[39] The unambiguous results obtained from this system contrast with those for the C−T system, where the authors acknowledged their "inability to distinguish between" the symmetric and asymmetric structures.[12]

Table 1. Important Bond Distances (Å)

		1	2	3
unit 1	Mo(1)−Mo(2)	2.0898(5)	2.105(1)	2.1306(3)
	Mo−N_{linker}	2.168(3)	2.143(9)	2.114(2)
	Mo−O_{linker}	2.114(3)	2.064(8)	2.025(2)
	Mo−N_{DAniF} (cis)	2.158(4)	2.148(9)	2.130(3)
	Mo−N_{DAniF} (trans)	2.130(4)	2.120(9)	2.118(2)
unit 2	Mo(3)−Mo(4)	2.0910(5)	2.112(1)	
	Mo−N_{linker}	2.177(3)	2.14(1)	
	Mo−O_{linker}	2.096(2)	2.047(7)	
	Mo−N_{DAniF} (cis)	2.151 (4)	2.133(9)	
	Mo−N_{DAniF} (trans)	2.131 (3)	2.122(9)	

Near-IR Spectra. The spectrum of **2** in a dichloromethane solution (Figure 4), in the 800−3000 nm region, shows a relatively intense band with a molar absorptivity of 1.2 × 10^4 mol^{-1} cm^{-1} centered at 4940 cm^{-1}. The corresponding band is observed at 4980 cm^{-1} in acetone solution and at 4880 cm^{-1} in THF solution. No band occurs in this region in the spectra of **1** and **3**. The observed bandwith, $\Delta\nu_{1/2}$ = 1172 cm^{-1}, is

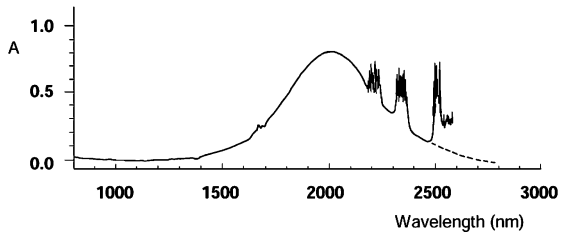

Figure 4. Near-IR spectrum of the mixed-valence species **2** in CH_2Cl_2. Narrow solvent vibrational overtone bands appear at low energy.

(38) In systems other than THF/hexanes, e.g., diffusion of hexanes into either dichloromethane or dichloroethane solutions, crystals of **2** having the molecule in a monoclinic space group, $P2_1/c$, were obtained in which the structure of the core appears to be flat due to crystallographic disorder. Consequently, the bond distances, whether intrinsically equal or not, appear to be equal. For **2**·$2CH_2ClCH_2Cl$, a = 17.303(1), b = 17.590(1), and c = 36.537(1) Å, β = 96.952(2)°; Mo(1)−Mo(2) = 2.11(1) Å, Mo(3)−Mo(4) = 2.12(1) Å.

(39) To our knowledge, this is the only known example in which the neutral, singly oxidized, and doubly oxidized species have been structurally characterized.

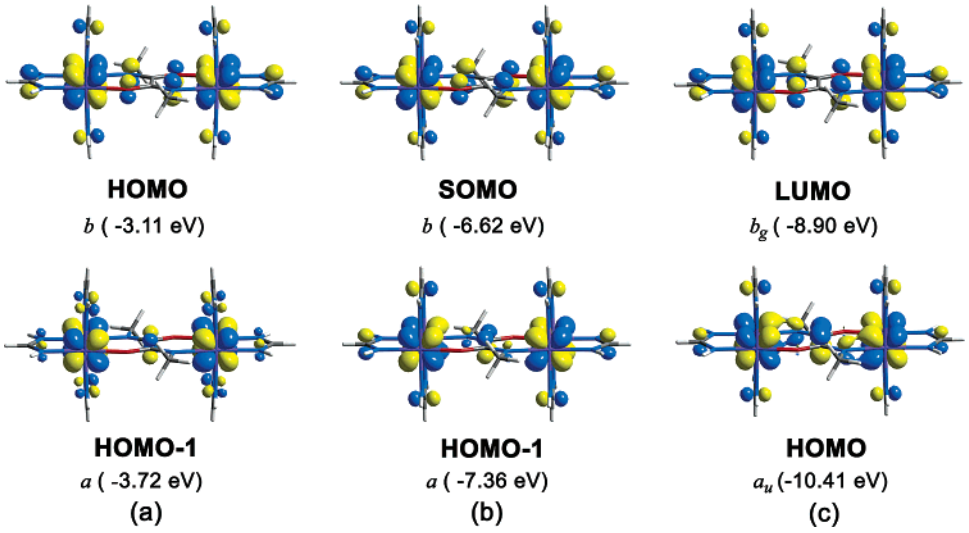

Figure 5. The 0.04 surface contour diagrams for the two highest occupied molecular orbitals for models of **1**, **2**, and **3**, calculated by DFT.

significantly less than the 3380 cm^{-1} predicted for a MV intervalence transition for a class II system using the Hush formula, $\Delta\nu_{1/2} = (2310\nu_{max})^{1/2}$ cm^{-1}. The existence of this relatively narrow and solvent-independent band in the near-infrared region suggests that the MV compound **2** should be classified as being at or beyond the border between classes II and III.[22d,40] These results are consistent with those for the β-oxamidate-bridged compounds in which the methyl groups were replaced by aryl substituents such as phenyl and anisyl groups.[19]

Electronic Structure and DFT Calculations. To obtain further insight into the electronic structure and into the effect of the conformation on electron delocalization, a series of DFT calculations was carried out. A specific goal was to determine whether the increasing planarity of the unit composed of the two Mo−Mo bonds and the linker on going from the unoxidized **1** to the doubly oxidized **3** is caused by intrinsic electronic effects or is only an adventitious result of packing forces. The calculations were performed on a model molecule in which all anisyl groups were replaced by hydrogen atoms; previous work on analogous models has yielded satisfactory results.[19] Geometry optimizations of three models, one each for the neutral, singly oxidized, and doubly oxidized species, were done on the basis of the starting parameters from the crystal structures of **1**, **2**, and **3**, respectively.

A comparison of the MOs of the different models (Figure 5) shows that the electronic structures are, as expected, similar to one another. The MOs for the neutral model having C_2 symmetry, Figure 5a, resemble those of the phenyl-substituted oxamidato compound,[19] with the HOMO having *b* symmetry. This corresponds to the out-of-phase combination of the δ orbitals with a nonbonding π orbital of the linker in an antibonding fashion; a diagram of this interaction is shown in Figure 6. Additionally, the HOMO−1, which has *a* symmetry, is obtained by the in-phase combination of the δ orbitals with an empty π^* orbital from the ligand. The *a* combination is a vehicle for back-bonding interactions from the filled metal orbitals to the ligand, which stabilize the system. In addition,

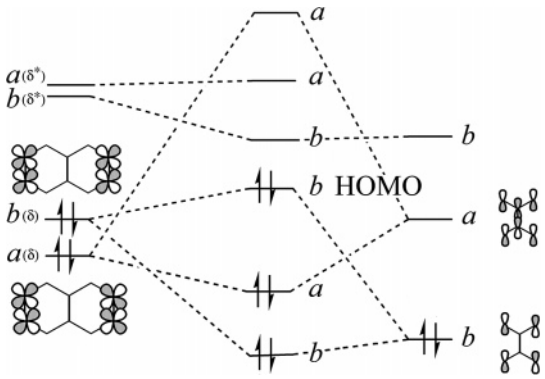

Figure 6. Frontier orbital interactions between the Mo_2 (δ) units and linker (π) for a system with a strong antiferromagnetic interaction.

the optimized geometry of the neutral model starting from the crystal structure parameters showed a distortion from planarity qualitatively similar to that of the structure of **1**. However, results of a geometry optimization starting from a planar geometry favor the planar geometry, as its total energy is lower than that of the nonplanar model.

In general, the results for the electronic structure of the singly oxidized C_2 model of **2** are similar to those in the N-aryl case.[19] The unpaired electron resides in the *b* orbital, as shown in Figure 5b. Again, the optimized geometry of the relaxed, singly oxidized model is planar. This suggests that the degree of planarity in the structure depends on steric effects. It should be mentioned that the amount of ligand character in the SOMO is significant (32%); an electron in this orbital can be described as delocalized.

The model for **3**, which is doubly oxidized, may be described by two different spin states. A high-spin model ($S = 1$) would be appropriate for a system where the frontier orbitals show little or no significant overlap between the dimetal units and the bridge ligand. This would represent two dimetal units independent from each other, but it conflicts with the electrochemical data (vide infra). Conversely, a low-spin model ($S = 0$), appropriate for a system in which the overlap between the orbitals of the dimetal units and the bridge ligand is extensive, would represent a case in which strong antiferromagnetic coupling (hence, electronic communication) is present. Initially, two different single-point calculations, at the geometry of the

(40) See for example: (a) Hush, N. S. *Coord. Chem. Rev.* **1985**, *64*, 135. (b) Laye, R. H.; Couchman, S. M.; Ward, M. W. *Inorg. Chem.* **2001**, *40*, 4089. (c) Scheiring, T.; Kaim, W.; Olabe, J. A.; Parise, A. R.; Fiedler, J. *Inorg. Chim. Acta* **2000**, *300*−*302*, 125.

Table 2. Results from DFT Calculations

model	charge	total spin, *S*	energy[a] (a.u.)	calculated bond lengths, Å: Mo–Mo	C–C
1	0	0	−1582.8786	2.1349	1.5109
				2.0898(5)[b]	1.518(5)[b]
2	+1	$^1/_2$	−1582.7237	2.1513	1.4958
				2.105(1)[c]	1.522(12)[c]
3	+2	0	−1582.4382	2.1692	1.4802
3	+2	1	−1582.4362	2.1645	1.5277
			Δ−0.05 eV	2.1306(3)[d]	1.508(5)[d]
3	+2	0	−1582.8774[e]		
3	+2	1	−1582.8603[e]		
			Δ−0.46 eV		

[a] Geometry optimization energies obtained with the B3LYP functional unless otherwise noted. [b] Experimental value for **1**. [c] Experimental value for **2**. [d] Experimental value for **3**. [e] Single point energy values obtained with the BP86 functional at the optimized geometry of **3**.

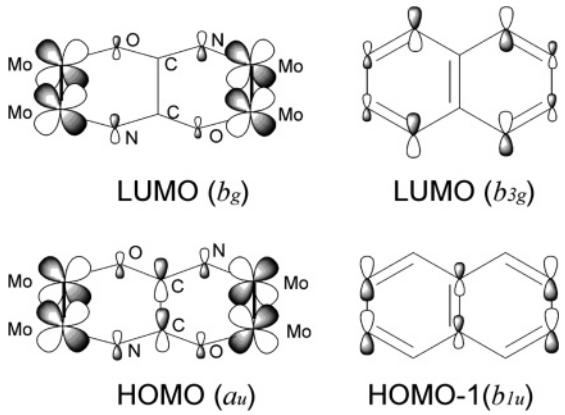

Figure 7. Diagram of the frontier orbitals for **3** (left) and naphthalene (right).

crystal structure, were performed with the purpose of finding the relative energies of the two spin states. A restricted[41] singlet calculation and an unrestricted triplet calculation were performed. As presented in Table 2, the singlet state is favored by 0.2 eV (1613 cm^{-1}). Nevertheless, to examine this situation further, geometry optimizations were performed for both spin states. Again the results favor the singlet state, though by only 0.05 eV (403 cm^{-1}).

Because the amount of Hartree−Fock exchange in the hybrid functional B3LYP is known to favor higher multiplicities, the energy difference between the singlet and triplet indicated by such a calculation is likely to be an underestimate.[42] For this reason, a pure density functional (BP86), which does not incorporate Hartree−Fock exchange, was also used to calculate the energy difference between the singlet and triplet states at the B3LYP-optimized geometries. This calculation places the $S = 0$ state 0.46 eV (3743 cm^{-1}) below the $S = 1$ state.

Furthermore, the broken symmetry (BS) approach[43] has been found to yield accurate results in estimating the Heisenberg exchange coupling constants, $2J$.[44] Moreover, Bénard and coworkers[45] have shown that, by applying Yamaguchi's relation,[46,47] this method can be successfully utilized for calculating such coupling constants in metal−metal bonded species. Breaking the symmetry of the wave function using this method in the B3LYP-optimized singlet model for **3** increased the energy difference from the respective triplet state by 0.06 eV. The calculated spin eigenvalue for the BS solution, $\langle S_{BS}^2 \rangle = 0.5411$, indicates a relatively small amount of spin contamination in the wave function. This suggests that there is considerable overlap between the orbitals in the two dimetal units.[43] The value found for the coupling constant, $2J$, by utilizing Yamaguchi's relation is −1236 cm^{-1}. Applying the BS approach to the wave function obtained by the BP86 functional did not change the energy difference. This suggests that the true $2J$ value is in the range between that obtained through the broken symmetry method and the energy difference of the singlet and triplet states obtained by the BP86 functional, namely between −1236 and −3743 cm^{-1}. Negative values of $2J$ larger than 800 cm^{-1} should lead to diamagnetism,[9c] and thus, these results are consistent with the measured temperature-independent diamagnetism of **3** (below 300 K) (vide infra). Thus, our analysis of the electronic structure led us to conclude that the triplet model represents an excited state relative to the singlet case. The singlet model has paired electrons in the a_u orbital, and the triplet model accommodates one electron in the a_u and one in the higher-lying b_g orbital.

As in the crystal, the optimized geometry (for both the singlet and the triplet states) is planar, with calculated torsion angles of zero along the junction of the two six-membered rings formed by the linker and the two Mo_2 units. This implies that the metal orbitals are integrated into a π system which is continuous over the ligand and metal orbitals,[48] and the core of **3** has the appearance of a heteronaphthalene. This continuity of the π system provides effective electronic communication between metal centers.[1d,2a] The resemblance of this bicyclic ring system to that of naphthalene[49] is quite remarkable, as emphasized by comparison of the frontier MOs of the aromatic system in naphthalene, D_{2h}, and those of the β-oxamidate-bridged compounds which are depicted in Figure 7. The naphthalene LUMO (b_{3g}) and the HOMO−1 (b_{1u}) are very similar in their nodal structure to the *b* and *a* orbitals in the series of oxamidate species.

Previous theoretical work on similar compounds[13c] has shown that time-dependent density functional theory (TD-DFT) calculations are useful in the assignment of electronic spectra. For **2**, a near-IR transition is observed as a broad and intense band centered at about 2025 nm. This band might be assigned to an intervalence transition, as mentioned in the previous section. However, a TD-DFT calculation on the model for **2** shows that

(41) Following the suggestion of a reviewer, an $S = 0$ unrestricted geometry optimization for the model of **3** was also performed. The resulting geometrical parameters between the two calculations were essentially identical.
(42) Reiher, M.; Salomon, O.; Hess, B. A. *Theor. Chem. Acc.* **2001**, *107*, 48.
(43) Illas, F.; Moreira, I.; Graaf, C.; Barone, V. *Theor. Chem. Acc.* **2000**, *104*, 265.
(44) (a) Noodleman, L. *J. Chem. Phys.* **1981**, *74*, 5737. (b) Noodleman, L.; Davidson, E. R. *Chem. Phys.* **1986**, *109*, 131. (c) Sinnecker, S.; Neese, F.; Noodleman, L.; Lubitz, W. *J. Am. Chem. Soc.* **2004**, *126*, 2613.
(45) Kiehl, P.; Rohmer, M.-M.; Bénard, M. *Inorg. Chem.* **2004**, *43*, 3151.
(46) Soda, T.; Kitagawa, Y.; Onishi, T.; Takano, Y.; Shigeta, Y.; Nagao, H.; Yoshioka, Y.; Yamaguchi, K. *Chem. Phys. Lett.* **2000**, *319*, 223.
(47) Yamaguchi's method for calculating J is provided by the following equation: $J = -E_{HS} - E_{BS}/\langle S_{HS}^2 \rangle - \langle S_{BS}^2 \rangle$, where E_{HS} and E_{BS} are the total energy of the high-spin calculation (triplet in our case) and the total energy of the broken symmetry calculation, respectively, and $\langle S_{HS}^2 \rangle$ and $\langle S_{BS}^2 \rangle$ represent the total spin angular momentum for the high-spin (triplet) and broken symmetry cases, respectively. The exchange coupling parameter, J, is based on the Heisenberg−Dirac−van Vleck spin (HDVV) Hamiltonian: $\mathbf{H} = -2JS_1S_2$.
(48) Conjugation of the π system of linkers and orbitals of dimolybdenum units has been documented in compounds having $[Mo_2]$ species connected by polyunsaturated dicarboxylate anions. See ref 13 b.
(49) Cotton, F. A. *Chemical Applications of Group Theory*, 3rd ed.; Wiley-Interscience: New York, 1990; p 172.

Table 3. Some Oxidation Potentials and Comproportionation Constants for $[Mo_2]$(linker)$[Mo_2]$

linker	$[Mo_2]$–$[Mo_2]$	$[Mo_2]\cdots[Mo_2]$ (Å)	$E_{1/2}^{+/0}$ (mV)	$E_{1/2}^{2+/+}$ (mV)	$\Delta E_{1/2}$ (mV)	K_c	re
SO_4^{2-}	⊥	6.010	93	321	228	7.2×10^3	14
$Zn(OMe)_4^{2-}$	⊥	6.548	−208	4	212	3.8×10^3	20
$Co(OMe)_4^{2-}$	⊥	6.562	−211	−4	207	3.2×10^3	20
α-diphenyloxamidate	⊥	7.096	176	367	191	1.7×10^3	19
α-dianisyloxamidate	⊥	7.081	183	373	190	1.6×10^3	19
oxalate	∥	6.953	294	506	212	3.8×10^3	13b
β-diphenyloxamidate	∥	6.322	−157	383	540	1.3×10^9	19
β-dianisyloxamidate	∥	6.334	−196	327	523	6.9×10^8	19
β-dimethyloxamidate	∥	6.248	−169	362	531	9.5×10^8	this work

a HOMO−1 → SOMO transition can account for this band. The calculated wavelength (nm) and oscillator strength (*f*) are 1215 and 0.206, respectively, both comparable to the experimental values. Thus, in this case, the term "intervalence charge-transfer band" is not the best description for this near-IR transition, which does not show any pronounced transference of charge from one redox site to the other. It is best described as a dipole-allowed HOMO−1 → SOMO electronic transition.

Magnetic Studies. As mentioned earlier, **1** is diamagnetic, as inferred from the sharpness of most of the ^{1}H NMR signals and as expected from the presence of two $\sigma^2\pi^4\delta^2$ quadruply bonded Mo_2^{4+} units in which all electrons are paired. For the doubly oxidized **3** there are several possibilities that would give different magnetic behaviors. It is most unlikely that two electrons could be removed from only one of the units so that one Mo_2 unit would have a $\sigma^2\pi^4\delta^0$ configuration and the other one a $\sigma^2\pi^4\delta^2$ configuration. This situation could not be the ground state in a system that is strongly coupled, and it is inconsistent with the presence of equivalent Mo−Mo bond lengths.

The loss of one electron by each of the $[Mo_2]$ units, which would give each one a $\sigma^2\pi^4\delta^1$ electronic configuration, is supported by the structural evidence. As described in the previous section, the magnetic behavior of the dication $[Mo_2]^+$L-$[Mo_2]^+$, which has one unpaired electron at each dimetal center, is determined by the sign and the magnitude of the energy difference, 2*J*, between an electron spin singlet state and a triplet state. If the 2*J* value is very small or zero, the system would have negligible magnetic exchange interaction, a situation already encountered in $(DAniF)_3Mo_2(MeO)_2Zn(MeO)_2Mo_2$-$(DAniF)_3$.[20b] Variable-temperature magnetic measurements (Figure S2) on a crystalline sample of **3** are consistent with the results of DFT calculations and show that, within experimental error, the values of χT are essentially zero in the temperature range from 5 to 300 K. The strong antiferromagnetic exchange coupling between the two Mo_2^{5+} units results from the great electronic coupling provided by the oxamidate linker in its *β* form. This means that 2*J* is negative in sign and exceeds 3*kT* at 300 K.

EPR Spectrum and Magnetism for 2. The X-band (9.5 GHz) electron paramagnetic resonance spectrum (EPR) of the singly oxidized **2** in frozen CH_2Cl_2 solution (Figure S3) exhibits a highly symmetric signal devoid of hyperfine structure, and having $g_{iso} = 1.9443 \pm 0.0003$, which is consistent with an electronic ground state having $S = {}^1/_2$. The *g* value is significantly lower than that of a free radical because of spin−orbit coupling in the $[Mo_2]$ units. This indicates that the unpaired electron resides in an orbital of principally metal character. This signal is attributed to the ^{96}Mo ($I = 0$) isotope from the $[Mo_2]$ units, and the *g* value is similar to those in other compounds with an Mo_2^{5+} core.[16,50] In a prior study, it was found that two MV compounds of this type, $[Mo_2]M(OCH_3)_4[Mo_2]^+$ (M = Zn, Co), have EPR signals with hyperfine structure of the sort expected for dinuclear Mo_2^{5+} species, because in each compound there are localized Mo_2^{4+} and Mo_2^{5+} units.[20b] The absence of hyperfine structure in **2**, as was also observed in the compound having an $[Mo_2]^{0.5+}(\mu\text{-}Cl_4)[Mo_2]^{0.5+}$ core, is reasonable. For a tetranuclear $[Mo_2]L[Mo_2]$ species, there are 21 magnetically dissimilar species with a naturally occurring isotope composition. With so many isotopomers, the superimposed hyperfine satellites are not resolvable at the X-band frequency (9.5 GHz). The EPR signals are expected to be averaged in the delocalized case (EPR time scale of 10^{-5}−10^{-9} s). Similarly, hyperfine coupling in the EPR spectra of the C−T ion has not been observed.[51] The χT value of 0.35 emu K mol^{-1} for **2** in the range of 5−300 K is slightly lower than the calculated value of 0.375 for a system with one unpaired electron ($S = {}^1/_2$) and $g = 2.00$. When the experimental *g* value (1.9443) from the EPR spectrum of **2** is used,[52] there is excellent agreement ($\chi T = 0.354$ emu K mol^{-1}) with the experimental result.

Electrochemistry. Both the cyclic voltammogram (CV) and differential pulse voltammogram (DPV) of **1** have two well-separated redox waves (Figure 8). The first oxidation ($E_{1/2}^{+/0}$),

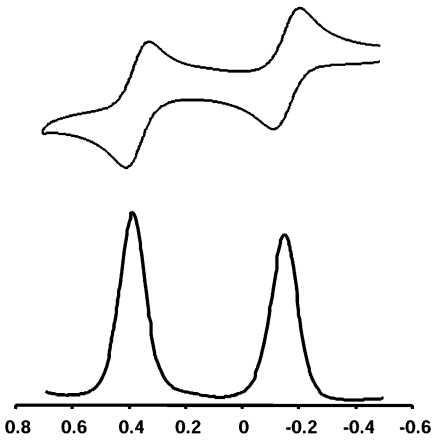

Figure 8. Cyclic voltammogram (CV with potentials vs Ag/AgCl) and differential pulse voltammogram (DPV) for **1** in CH_2Cl_2 solution at ca. 22 °C.

which yields a singly charged species, occurs at −169 mV versus Ag/AgCl, and the second one ($E_{1/2}^{2+/+}$) at 362 mV

(50) (a) Cotton, F. A.; Frenz, B. A.; Pedersen, E.; Webb, T. R. *Inorg. Chem.* **1975**, *14*, 391. (b) Cotton, F. A.; Pedersen, E. *Inorg. Chem.* **1975**, *14*, 399.
(51) (a) Bunker, B. C.; Drago, R. S.; Hendrickson, D. N.; Richman, R. M.; Kessell, S. L. *J. Am. Chem. Soc.* **1978**, *100*, 3805. (b) Stebler, A.; Ammeter, J. H.; Fürholz, U.; Ludi, A. *Inorg. Chem.* **1984**, *23*, 2764.

generates the doubly charged species. These values are similar to those for the β isomers of two diaryloxamidates reported earlier and shown in Table 3, along with other analogues. For the dicarboxylate analogues the oxidation potentials are around 200−300 mV. Thus, the β-type oxamidate-linked compounds are relatively easy to oxidize because the HOMO is at higher energy compared to the carboxylate analogues. Furthermore, the $\Delta E_{1/2}$ value of 531 mV for **1** is much larger than that (212 mV) found in the oxalate compound. These values bracket that of 360 mV for the C−T complex.[5b]

Using the $\Delta E_{1/2}$ value,[17] $K_C = 9.5 \times 10^8$ is obtained. This is significantly larger than that of 10^6 for the C−T ion.[2a] This also suggests that the MV species **2** should be assigned to class III.[7] This is remarkable as all $[Mo_2]L[Mo_2]$ compounds with dicarboxylate linkers are only weakly or at best moderately coupled, and thus assigned to either class I or class II. The strong electronic communication evidenced by electrochemical measurements is consistent with the results of DFT calculations described above.

4. Concluding Remarks

The study of three redox-related species, $[Mo_2]$(oxamidate)-$[Mo_2]^{n+}$ (n = 0, 1, and 2), has demonstrated that the β coordination mode of the oxamidate linker provides an effective pathway for electronic coupling between dimolydenum units. Thus, the singly oxidized **2** can be assigned to a mixed-valence species of class III. This is supported by experimental data from crystallography, electrochemistry, electronic spectra, and magnetism. It is notable that the doubly oxidized compound **3** is diamagnetic and has a singlet (S = 0) ground state, which is a manifestation of metal−metal antiferromagnetic interaction between the two $[Mo_2]$ units. The singlet ground state for **3** is consistent with results from DFT calculations.

Further studies with other techniques having different time scales, such as Raman and photoelectron spectroscopies as well as more detailed electronic spectral studies and high field EPR, are being considered for these and other analogous systems.

Acknowledgment. We thank the National Science Foundation, the Robert A. Welch Foundation, and Texas A&M University (through the Laboratory for Molecular Structure and Bonding) for financial support and Mr. C. Fewox for assistance with EPR measurements. We also thank Prof. M. B. Hall, Dr. L. M. Pérez, and Dr. C. E. Webster for helpful discussions on the DFT calculations and the Laboratory for Molecular Simulation for software.

Supporting Information Available: X-ray crystallographic data in CIF format for **1**·4CH_2ClCH_2Cl, **2**·6THF, and **3**·3CH_2Cl_2; tables of selected crystallographic data and bond distances and angles (Tables S1 and S2, respectively), a displacement ellipsoid plot of the cation in **2**·6THF (Figure S1), a plot of the temperature dependence of the magnetic susceptibility of paramagmetic compound **2** and diamagnetic compound **3** (Figure S2), X-band EPR spectrum of **2** (Figure S3), and drawings of δ and δ*, metal-based MOs from the DFT calculations for models of **1** and the cations in **2** and **3** (Figure S4), in PDF. This material is available free of charge via the Internet at http://pubs.acs.org.

JA046775F

(52) According to Curie's law, $\chi_m = Ng^2\beta^2/3kT \cdot S(S+1)$, $\chi_m T = Ng^2\beta^2/3k \cdot S(S+1) \approx 1/8 \cdot g^2 S(S+1)$.